# Synthesis and Characterization of a Family of Thioether-Dithiolate-Bridged Heteronuclear Iron Complexes

**Yahui Zhang,[a] Dawei Yang,*[,a] Ying Li,[a] Baomin Wang,[a] Xiangyu Zhao[a] and Jingping Qu*[,a,b]**

[a]State Key Laboratory of Fine Chemicals, Dalian University of Technology, 2 Linggong Road, Dalian, 116024, P.R. China.

[b]Key Laboratory for Advanced Materials, East China University of Science and Technology, Shanghai, 200237, P.R. China.

* E-mail: qujp@dlut.edu.cn
yangdw@dlut.edu.cn

**Contents:**

Table **S**1. Crystal data and structure refinement for complexes **2**, **3** and **4**

| Compound | **2** | **3** | **4** |
|---|---|---|---|
| Formula | $C_{28}H_{46}CoFe_2P_2F_{12}S_6$ | $C_{28}H_{46}NiFe_2P_2F_{12}S_6$ | $C_{36}H_{58}PdFe_2P_2F_{12}S_6N_4$ |
| Formula weight | 1035.58 | 1035.36 | 1247.26 |
| Crystal dimensions ($mm^3$) | 0.30 × 0.20 × 0.17 | 0.38 ×0.20×0.17 | 0.40 × 0.29 × 0.18 |
| Crystal system | Monoclinic | Monoclinic | Orthorhombic |
| Space group | P2(1)/c | P2(1)/c | Fdd2 |
| a (Å) | 39.9194(12) | 39.3157(14) | 16.8637(16) |
| b (Å) | 11.8698(3) | 11.8932(5) | 52.655(6) |
| c (Å) | 18.0617(6) | 18.1269(6) | 11.3865(16) |
| $\alpha$ (°) | 90.00 | 90.00 | 90.00 |
| $\beta$ (°) | 91.9193(12) | 92.5325(13) | 90.00 |
| $\gamma$ (°) | 90.00 | 90.00 | 90.00 |
| Volume ($Å^3$) | 8553.5(4) | 8467.7(5) | 10111(2) |
| Z | 8 | 8 | 8 |
| T (K) | 173(2) | 173(2) | 293(2) |
| $D_{calcd}$ ($g\ cm^{-3}$) | 1.608 | 1.624 | 1.639 |
| $\mu$ ($mm^{-1}$) | 1.494 | 1.562 | 1.305 |
| $F$ (000) | 4216 | 4224 | 5072 |
| No. of rflns. collected | 147304 | 134599 | 16340 |
| No. of indep. rflns. /$R_{int}$ | 15051 / 0.0412 | 14898 / 0.0397 | 5765 / 0.0385 |
| No. of obsd. rflns. [$I_0 > 2\sigma(I_0)$] | 12794 | 13222 | 4849 |
| Data / restraints / parameters | 15051 / 1/ 965 | 14898 / 1171 / 975 | 5765/ 1 / 288 |
| $R_1$ / $wR_2$ [$I_0 > 2\sigma(I_0)$] | 0.0412 / 0.1111 | 0.0360/ 0.0938 | 0.0316 / 0.0665 |
| $R_1$ / $wR_2$ (all data) | 0.0533 / 0.1158 | 0.0429 / 0.0967 | 0.0422 / 0.0710 |
| GOF (on $F^2$) | 1.197 | 1.115 | 1.008 |
| Largest diff. peak and hole (e $Å^{-3}$) | 0.955 / −0.822 | 1.032 / −0.651 | 0.331 / −0.333 |
| CCDC No. | 1431984 | 1414699 | 1414702 |

**Table S2.** Crystal data and structure refinement for complexes **5**, **6** and **7**

| Compound | **5** | **6** | **7** |
|---|---|---|---|
| Formula | $C_{29}H_{48}CuFe_2Cl_2PF_6S_6$ | $C_{28}H_{46}AgFe_2PF_6S_6$ | $C_{32}H_{38}AuFeP_2F_6S_3$ |
| Formula weight | 980.14 | 939.55 | 947.56 |
| Crystal dimensions ($mm^3$) | 0.40 × 0.31 × 0.20 | 0.30 ×0.21×0.17 | 0.39 × 0.19 × 0.17 |
| Crystal system | Triclinic | Monoclinic | Orthorhombic |
| Space group | P-1 | P2(1)/n | P2(1)2(1)2(1) |
| a (Å) | 8.8586(6) | 14.408(2) | 12.9715(3) |
| b (Å) | 14.7856(7) | 16.545(2 | 13.7519(4) |
| c (Å) | 17.1123(10) | 16.329(2) | 20.3281(6) |
| $\alpha$ (°) | 66.542(3) | 90.00 | 90.00 |
| $\beta$ (°) | 78.470(4) | 108.902(2) | 90.00 |
| $\gamma$ (°) | 80.944(4) | 90.00 | 90.00 |
| Volume ($Å^3$) | 2007.1(2) | 3682.5(9) | 3626.18(17) |
| Z | 2 | 4 | 4 |
| T (K) | 296(2) | 296(2) | 296(2) |
| $D_{calcd}$ ($g\ cm^{-3}$) | 1.622 | 1.695 | 1.736 |
| $\mu$ ($mm^{-1}$) | 1.773 | 1.738 | 4.755 |
| $F$ (000) | 1004 | 1912 | 1868 |
| No. of rflns. collected | 12759 | 13532 | 19663 |
| No. of indep. rflns. /$R_{int}$ | 6988 / 0.0292 | 6463 / 0.0226 | 6356 / 0.0389 |
| No. of obsd. rflns. [$I_0 > 2\sigma(I_0)$] | 5716 | 5085 | 5456 |
| Data / restraints / parameters | 6988 / 385/ 569 | 6463 / 42 / 397 | 6356 / 0 / 291 |
| $R_1$ / $wR_2$ [$I_0 > 2\sigma(I_0)$] | 0.0640 / 0.1706 | 0.0512 / 0.1415 | 0.0313 / 0.0719 |
| $R_1$ / $wR_2$ (all data) | 0.0767/ 0.1786 | 0.0661 / 0.1512 | 0.0404 / 0.0754 |
| GOF (on $F^2$) | 1.121 | 1.066 | 0.984 |
| Largest diff. peak and hole (e $Å^{-3}$) | 1.064 / −1.305 | 1.012 / −1.333 | 1.323 / −0.428 |
| CCDC No. | 1414701 | 1414700 | 1414703 |

**Figure S1.** ORTEP diagram of **2**.

One of the two crystallographically independent molecules is shown. Thermal ellipsoids are shown at 50% probability level. Two $PF_6$ anions and all hydrogen atoms on carbons are omitted for clarity.

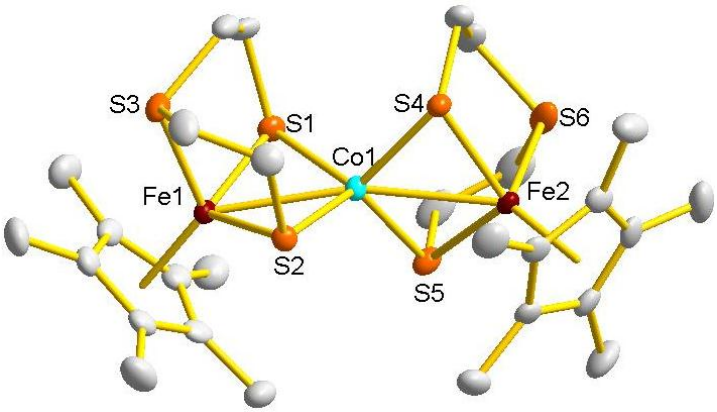


**Table S3.** Selected bond distances and angles for **2**.

| Distances (Å) | Molecule 1 | Molecule 2 | | Molecule 1 | Molecule 2 |
|---|---|---|---|---|---|
| Fe1–Co1 | 2.5765(7) | 2.5921(7) | Fe2–S6 | 2.233(1) | 2.234(1) |
| Fe2–Co1 | 2.5747(7) | 2.6117(7) | Co1–S1 | 2.197(1) | 2.206(1) |
| Fe1–S1 | 2.207(1) | 2.221(1) | Co1–S2 | 2.229(1) | 2.247(1) |
| Fe1–S2 | 2.225(1) | 2.231(1) | Co1–S4 | 2.203(1) | 2.211(1) |
| Fe1–S3 | 2.232 (1) | 2.238(1) | Co1–S5 | 2.220(1) | 2.223(1) |
| Fe2–S4 | 2.225(1) | 2.246(1) | Fe1–Cp*1 | 1.7593(5) | 1.7604(5) |
| Fe2–S5 | 2.213(1) | 2.202(1) | Fe2–Cp*2 | 1.7498(5) | 1.7519(5) |
| Angles (°) | Molecule 1 | Molecule 2 | | Molecule 1 | Molecule 2 |
| S1–Fe1–S2 | 105.83(4) | 106.56(4) | Co1–S4–Fe2 | 71.10(3) | 71.75(3) |
| S1–Fe1–S3 | 88.37(4) | 88.96(4) | S1–Co1–Fe2 | 134.18(3) | 139.06(3) |
| S4–Fe2–S5 | 106.29(4) | 105.62(4) | S4–Fe2–Co1 | 54.05(3) | 53.52(3) |
| S4–Fe2–S6 | 88.48(4) | 88.34(4) | S1–Fe1–Co1 | 54.03(3) | 55.01(3) |
| S1–Co1–S2 | 106.02(4) | 106.50(4) | Fe2–S5–Co1 | 71.01(3) | 72.34(3) |
| S1–Co1–S4 | 113.04(4) | 115.47(4) | Fe1–S2–Co1 | 70.68(3) | 71.50(3) |
| S4–Co1–S5 | 106.80(4) | 106.10(4) | Fe2–S4–Co1 | 71.10(3) | 71.75(3) |
| Fe1–S1–Co1 | 71.60(3) | 70.93(3) | Fe1–Co1–Fe2 | 165.58(3) | 158.37(3) |
| Torsion angles (°) | Molecule 1 | Molecule 2 | | Molecule 1 | Molecule 2 |
| S1–Fe1Co1–S2 | 157.84(5) | 160.60(5) | Cp*1–Cp*2 | 75.59(13) | 77.87(14) |
| S4–Fe2Co1–S5 | 160.01(4) | 161.17(5) | | | |

**Figure S2.** ORTEP diagram of **3**.

One of the two crystallographically independent molecules is shown. Thermal ellipsoids are shown at 50% probability level. Two $PF_6$ anions and all hydrogen atoms on carbons are omitted for clarity.

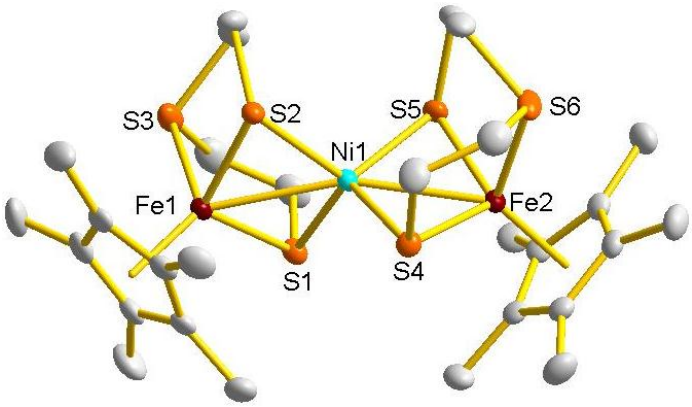


**Table S4.** Selected bond distances and angles for **3**.

| Distances (Å) | Molecule 1 | Molecule 2 | | Molecule 1 | Molecule 2 |
|---|---|---|---|---|---|
| Fe1–Ni1 | 2.560(2) | 2.550(2) | Fe2–S6 | 2.228(3) | 2.234(3) |
| Fe2–Ni1 | 2.543 (2) | 2.589(2) | Ni1–S1 | 2.218(3) | 2.241(2) |
| Fe1–S1 | 2.192(3) | 2.210(3) | Ni1–S2 | 2.189(3) | 2.193(3) |
| Fe1–S2 | 2.239(3) | 2.222(3) | Ni1–S4 | 2.239(2) | 2.212(3) |
| Fe1–S3 | 2.233(3) | 2.239(3) | Ni1–S5 | 2.183(3) | 2.205(2) |
| Fe2–S4 | 2.213(3) | 2.187(2) | Fe1–Cp*1 | 1.753(1) | 1.763 (1) |
| Fe2–S5 | 2.215(3) | 2.247(3) | Fe2–Cp*2 | 1.761(1) | 1.755(1) |
| Angles (°) | Molecule 1 | Molecule 2 | | Molecule 1 | Molecule 2 |
| S1–Fe1–S2 | 106.87(10) | 107.66(9) | S4–Ni1–Fe1 | 116.76(8) | 110.45(8) |
| S1–Fe1–S3 | 89.56(10) | 88.37(10) | Fe1–S1–Ni1 | 70.97(8) | 70.55(8) |
| S4–Fe2–S5 | 107.33(10) | 106.03(10) | Fe2–S4–Ni1 | 69.67(8) | 71.10(8) |
| S4–Fe2–S6 | 89.63(10) | 88.79(10) | S4–Fe2–Ni1 | 55.64(7) | 54.39(7) |
| S1–Ni1–S2 | 107.67(10) | 107.59(9) | S3–Fe1–Ni1 | 100.27(9) | 100.60(8) |
| S1–Ni1–S4 | 117.76(10) | 116.66(10) | S5–Ni1–Fe2 | 55.25(7) | 55.21(7) |
| S4–Ni1–S5 | 107.55(10) | 106.63(9) | S6–Fe2–Ni1 | 101.29(8) | 100.23(8) |
| S1–Ni1–Fe1 | 54.03(7) | 55.26(7) | Fe1–Ni1–Fe2 | 160.54(6) | 157.80(6) |
| Torsion angles(°) | Molecule 1 | Molecule 2 | | Molecule 1 | Molecule 2 |
| S1–Fe1Ni1–S2 | 162.13(12) | 161.24(11) | Cp*1–Cp*2 | 75.42(32) | 78.83(34) |
| S4–Fe2Ni1–S5 | 160.21(12) | 161.40(12) | | | |

**Figure S3.** ORTEP diagram of **4**.

Thermal ellipsoids are shown at 50% probability level. Two $PF_6$ anions and all hydrogen atoms on carbons are omitted for clarity.

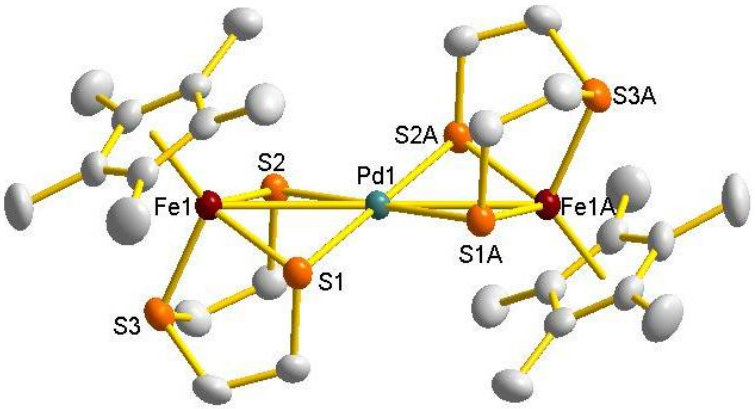


**Table S5.** Selected bond distances and angles for **4**.

| | | | |
|---|---|---|---|
| Distances (Å) | | | |
| Fe1–Pd1 | 2.9944(5) | Pd1–S2 | 2.352(1) |
| Fe1–S1 | 2.234 (1) | S1–C24 | 1.828(4) |
| Fe1–S2 | 2.232(1) | Fe1–C5 | 2.096(4) |
| Fe1–S3 | 2.2528(8) | Fe1–Cp*1 | 1.7502(4) |
| Pd1–S1 | 2.353(1) | | |
| Angles (°) | | | |
| S1–Fe1–S2 | 95.88(3) | Fe1–Pd1–Fe1A | 179.93(3) |
| S1–Fe1–S3 | 89.67(4) | S1–Fe1–Pd1 | 50.98(3) |
| S2–Fe1–S3 | 89.67(4) | S3–Fe1–Pd1 | 109.47(2) |
| S1–Pd1–S2 | 89.62(4) | Fe1–S1–Pd1 | 81.48(4) |
| S2–Pd1–S2A | 90.36(5) | Fe1–S2–Pd1 | 81.53(4) |
| S1–Pd1–Fe1 | 47.53(3) | Fe1–S2–C21 | 105.50(14) |
| S2–Pd1–Fe1 | 47.49(3) | | |
| Torsion angles (°) | | | |
| S1–Fe1Pd1–S2 | 145.75(5) | Cp*1–Cp*2 | 0.25(22) |

**Figure S4.** ORTEP diagram of **5**.

Thermal ellipsoids are shown at 50% probability level. One $PF_6$ anion and all hydrogen atoms on carbons are omitted for clarity.

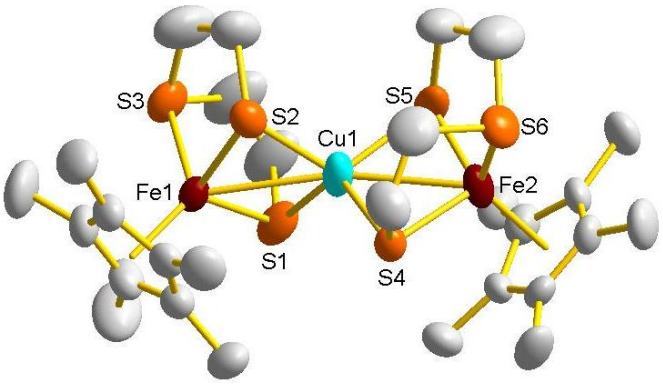


**Table S6.** Selected bond distances and angles for **5**.

| | | | |
|---|---|---|---|
| Distances (Å) | | | |
| Fe1–Cu1 | 2.766(1) | Fe2–S6 | 2.060(4) |
| Fe2–Cu1 | 2.747(1) | Cu1–S1 | 2.301(2) |
| Fe1–S1 | 2.252(2) | Cu1–S2 | 2.301(2) |
| Fe1–S2 | 2.257(2) | Cu1–S4 | 2.326(3) |
| Fe1–S3 | 2.226(2) | Cu1–S5 | 2.304(2) |
| Fe2–S4 | 2.172(3) | Fe1–Cp*1 | 1.748(1) |
| Fe2–S5 | 2.216(2) | Fe2–Cp*2 | 1.9040(8) |
| Angles (°) | | | |
| S1–Fe1–S2 | 104.61(7) | S4–Cu1–Fe1 | 115.53(9) |
| S1–Fe1–S3 | 88.50(7) | Fe1–S1–Cu1 | 74.80(6) |
| S4–Fe2–S5 | 108.06(10) | Fe2–S4–Cu1 | 75.18(10) |
| S4–Fe2–S6 | 96.4(2) | S3–Fe1–Cu1 | 99.99(6) |
| S1–Cu1–S2 | 101.63(7) | S5–Cu1–Fe2 | 51.13(5) |
| S1–Cu1–S4 | 106.72(13) | Fe1–Cu1–Fe2 | 165.31(4) |
| S4–Cu1–S5 | 100.15(10) | S1–Cu1–Fe1 | 51.79(4) |
| Torsion angles (°) | | | |
| S1–Fe1Cu1–S2 | 160.55(8) | Cp*1–Cp*2 | 78.21(45) |
| S4–Fe2Cu1–S5 | 167.64(14) | | |

**Figure S5.** ORTEP diagram of **6**.

Thermal ellipsoids are shown at 50% probability level. One $PF_6$ anion and all hydrogen atoms on carbons are omitted for clarity.

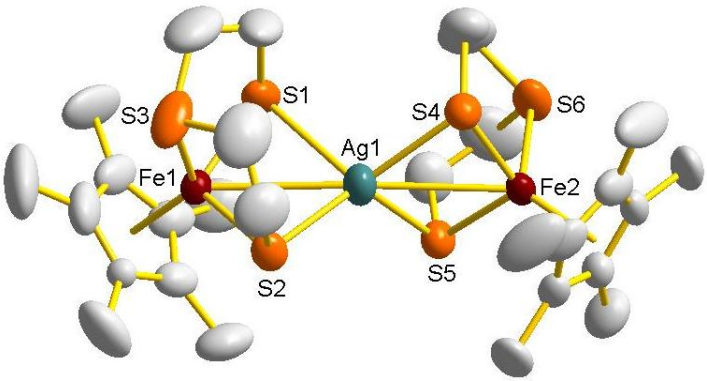


**Table S7.** Selected bond distances and angles for **6**.

| | | | |
|---|---|---|---|
| Distances (Å) | | | |
| Fe1–Ag1 | 3.0570(8) | Fe2–S6 | 2.215(2) |
| Fe2–Ag1 | 3.0689(8) | Ag1–S1 | 2.538(1) |
| Fe1–S1 | 2.267(2) | Ag1–S2 | 2.567(1) |
| Fe1–S2 | 2.273(1) | Ag1–S4 | 2.621 (2) |
| Fe1–S3 | 2.228(2) | Ag1–S5 | 2.488(1) |
| Fe2–S4 | 2.252(2) | Fe1–Cp*1 | 1.7528(6) |
| Fe2–S5 | 2.255(2) | Fe2–Cp*2 | 1.7553(8) |
| Angles (°) | | | |
| S1–Fe1–S2 | 107.69(6) | S4–Ag1–Fe1 | 131.78(4) |
| S1–Fe1–S3 | 88.15(6) | Fe1–S1–Ag1 | 78.79(4) |
| S4–Fe2–S5 | 106.96(6) | Fe2–S4–Ag1 | 77.66(5) |
| S4–Fe2–S6 | 88.62(8) | S1–Fe1–Ag1 | 54.54(4) |
| S1–Ag1–S2 | 91.78(5) | S3–Fe1–Ag1 | 100.12(5) |
| S1–Ag1–S4 | 108.23(5) | S5–Ag1–Fe2 | 46.45(3) |
| S4–Ag1–S5 | 90.24(5) | S6–Fe2–Ag1 | 101.42(5) |
| S1–Ag1–Fe1 | 46.67(3) | Fe1–Ag1–Fe2 | 170.94(3) |
| Torsion angles (°) | | | |
| S1–Fe1Ag1–S2 | 158.93(7) | Cp*1–Cp*2 | 63.83(24) |
| S4–Fe2Ag1–S5 | 161.54(7) | | |

**Figure S6.** ORTEP diagram of **7**.

Thermal ellipsoids are shown at 50% probability level. One $PF_6$ anion and all hydrogen atoms on carbons are omitted for clarity.

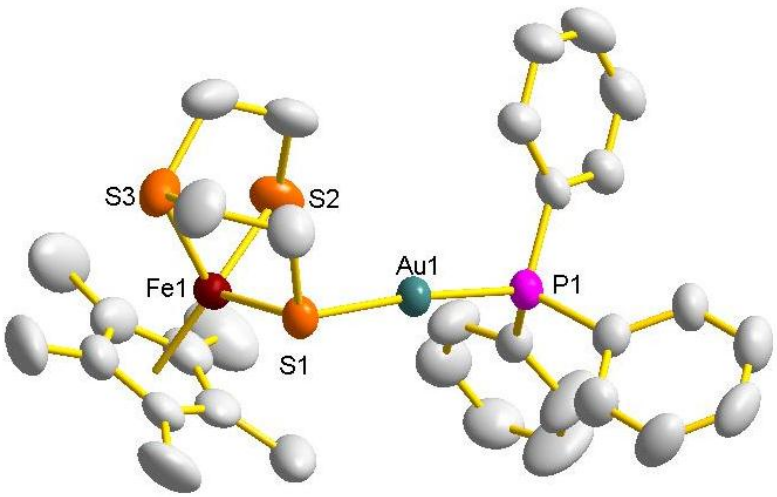


**Table S8.** Selected bond distances and angles for **7**.

| | | | |
|---|---|---|---|
| Distances (Å) | | | |
| Fe1–S1 | 2.298(1) | Au1–S1 | 2.3195 |
| Fe1–S2 | 2.207(1) | Au1–P1 | 2.261(1) |
| Fe1–S3 | 2.245(1) | Fe1–Cp* | 1.7499(9) |
| Angles (°) | | | |
| S1–Fe1–S2 | 102.7 | C1–Fe1–S3 | 139.19(6) |
| S1–Fe1–S3 | 87.8 | P1−Au2−S1 | 174.23(6) |
| S2–Fe1–S3 | 88.8 | | |

**Figure S7.** ESI-HRMS of **2** in $CH_2Cl_2$.

(a) The signal at an m/z = 372.4969 corresponds to **[2**−2$PF_6$**]**$^{2+}$. (b) Calculated isotopic distribution for **[2**−2$PF_6$**]**$^{2+}$ (upper) and the amplifying experimental diagram for **[2**−2$PF_6$**]**$^{2+}$ (bottom).

(a)

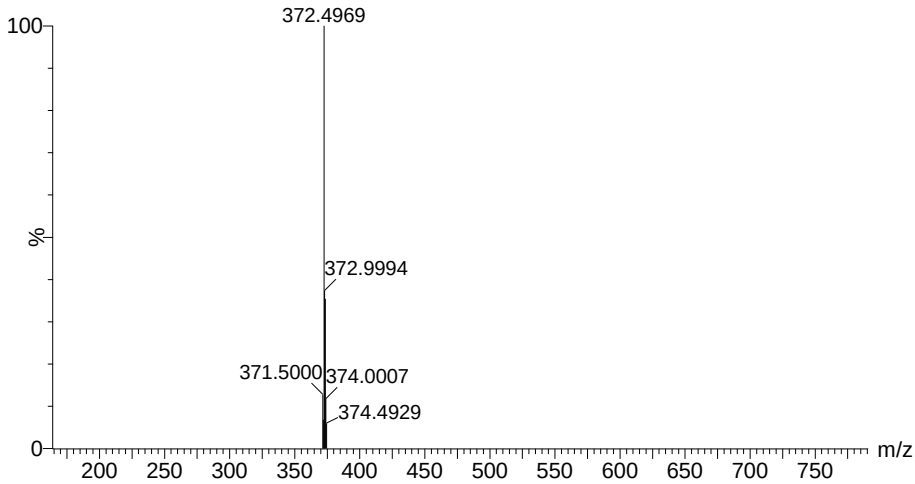


| | | | | | | |
|---|---|---|---|---|---|---|
| Minimum | | | | −1.5 | | |
| Maximum | | 5.0 | 5.0 | 100.0 | | |
| Mass | Calc. Mass | mDa | PPM | DBE | i−FIT | Formula |
| 744.9938 | 744.9955 | −1.7 | −2.3 | 6.0 | n/a | C28H46S6Fe2Co |

(b)

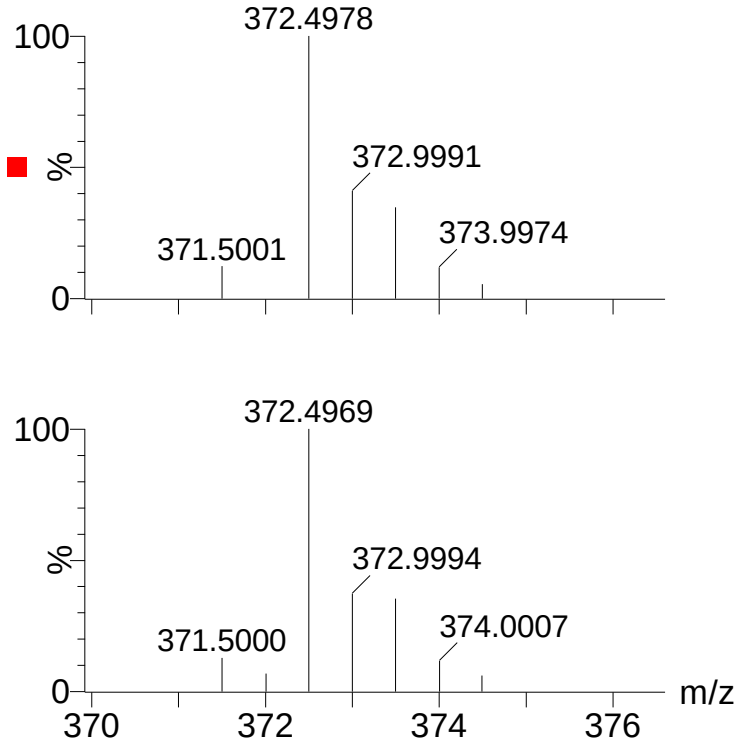

**Figure S8.** ESI-HRMS of **3** in $CH_2Cl_2$.

(a) The signal at an m/z = 371.9972 corresponds to **[3**−2$PF_6$**]**$^{2+}$, and the signal at an m/z = 888.8773 corresponds to **[3**−$PF_6$**]**$^{+}$. (b) Calculated isotopic distribution for **[3**−2$PF_6$**]**$^{2+}$ (upper) and the amplifying experimental diagram for **[3**−2$PF_6$**]**$^{2+}$ (bottom).

(a)

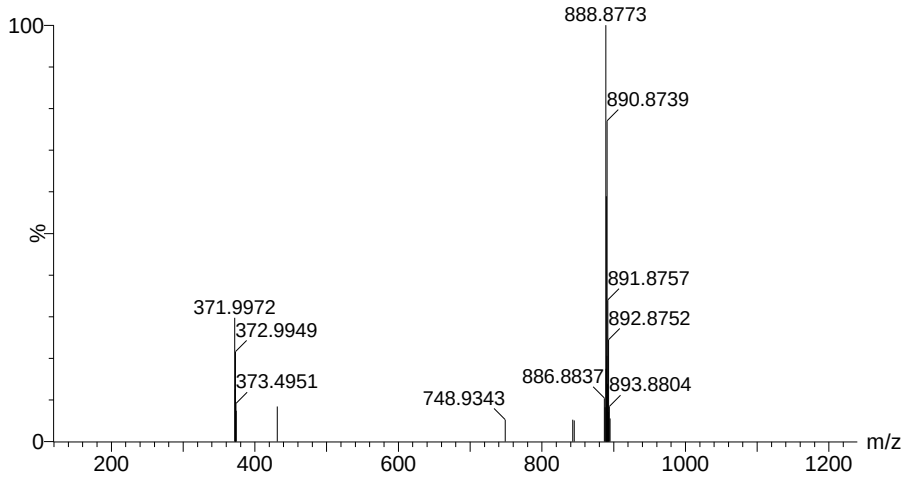


| | | | | | | |
|---|---|---|---|---|---|---|
| Minimum | | | | −1.5 | | |
| Maximum | | 5.0 | 5.0 | 50.0 | | |
| Mass | Calc. Mass | mDa | PPM | DBE | i−FIT | Formula |
| 743.9944 | 743.9976 | −3.2 | −4.3 | 6.5 | n/a | C28H46S6Fe2Ni |

(b)

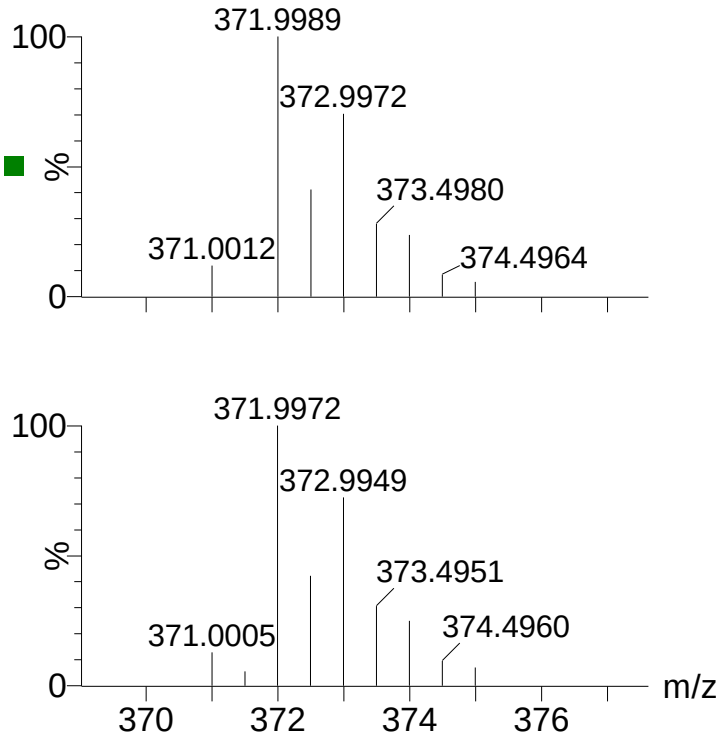

**Figure S9.** ESI-HRMS of **4** in $CH_3CN$.

(a) The signal at an m/z =395.9843 corresponds to **[4**−2$PF_6$**]**$^{2+}$. (b) Calculated isotopic distribution for **[4**−2$PF_6$**]**$^{2+}$ (upper) and the amplifying experimental diagram for **[4**−2$PF_6$**]**$^{2+}$ (bottom).

(a)

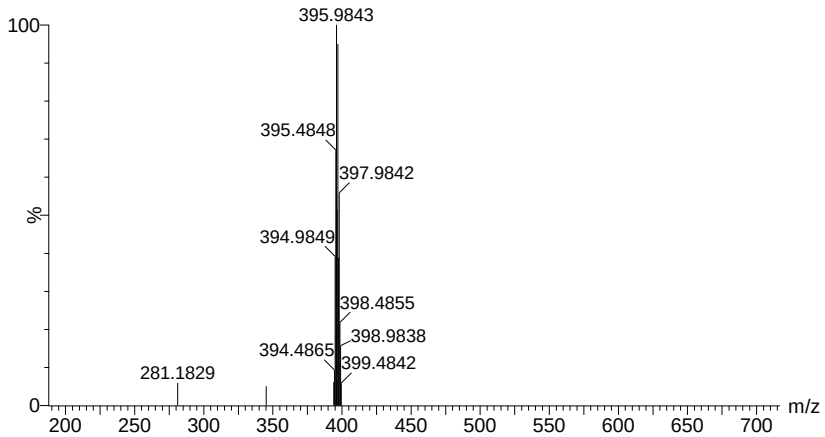


| | | | | | | |
|---|---|---|---|---|---|---|
| Minimum | | | | −1.5 | | |
| Maximum | | 5.0 | 5.0 | 100.0 | | |
| Mass | Calc. Mass | mDa | PPM | DBE | i−FIT | Formula |
| 791.9657 | 791.9657 | 2.9 | 3.7 | 6.0 | n/a | C28H46S6Fe2Pd |

(b)

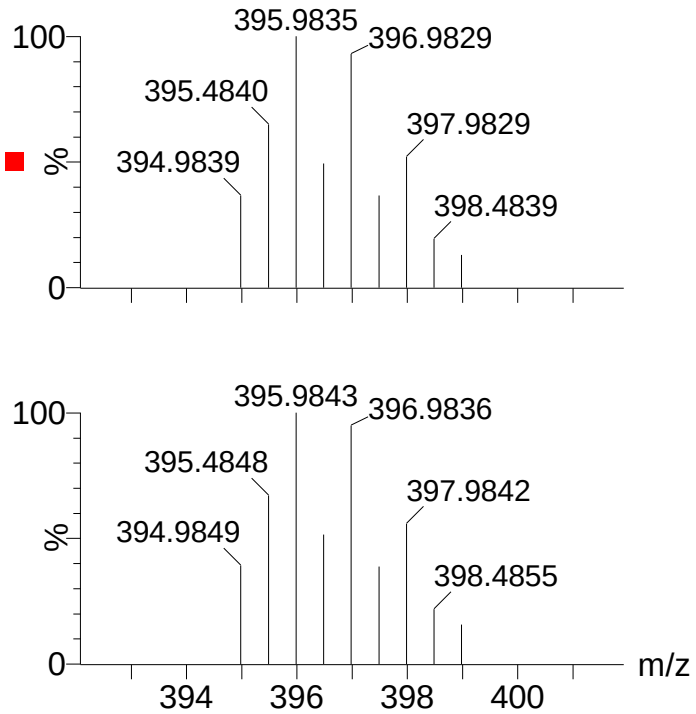

**Figure S10.** ESI-HRMS of **5** in $CH_2Cl_2$.

(a) The signal at an m/z = 748.9925 corresponds to **[5**−$PF_6$**]**$^+$. (b) Calculated isotopic distribution for **[5**−$PF_6$**]**$^+$ (upper) and the amplifying experimental diagram for **[5**−$PF_6$**]**$^+$ (bottom).

(a)

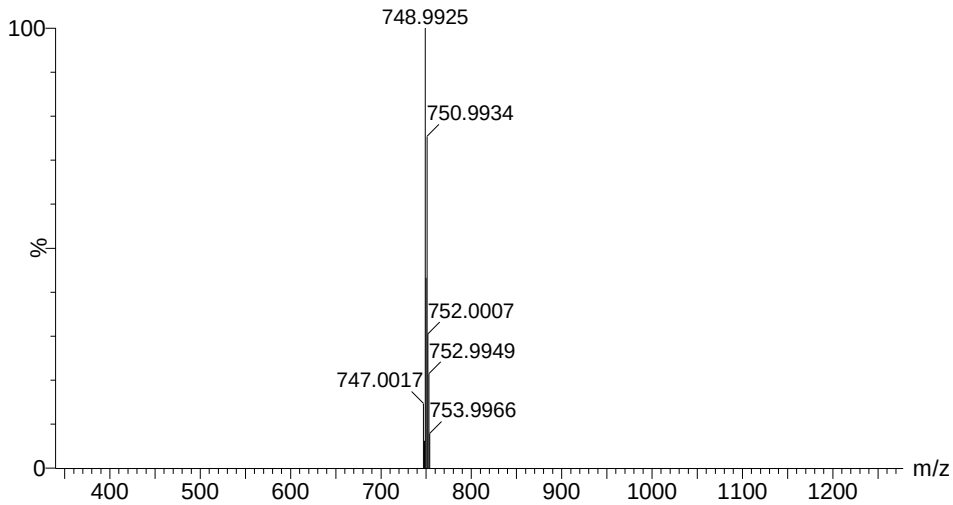


| | | | | | | |
|---|---|---|---|---|---|---|
| Minimum | | | | −1.5 | | |
| Maximum | | 5.0 | 5.0 | 100.0 | | |
| Mass | Calc. Mass | mDa | PPM | DBE | i−FIT | Formula |
| 748.9925 | 748.9919 | 0.6 | 0.8 | 6.0 | 2.1 | C28H46S6Fe2Cu |

(b)

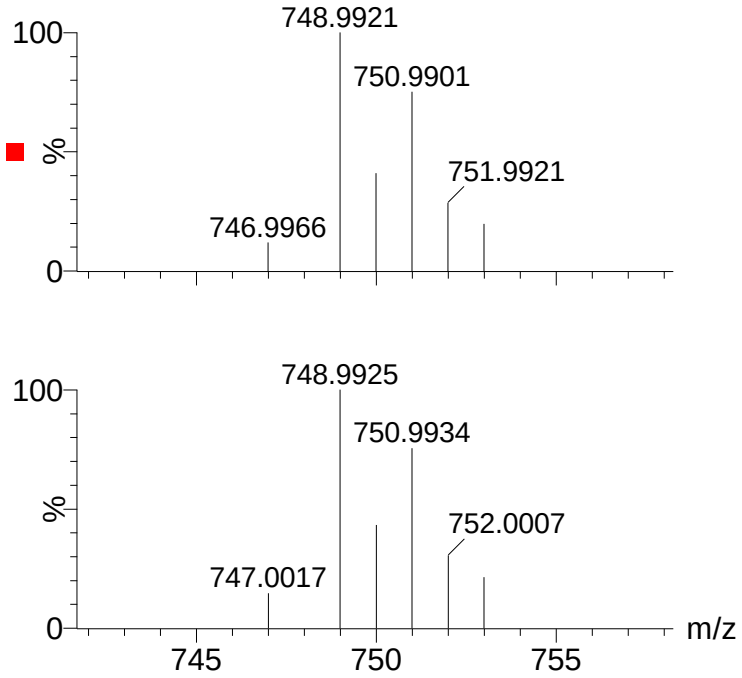

**Figure S11.** ESI-HRMS of **6** in $CH_2Cl_2$.

(a) The signal at an m/z = 794.9649 corresponds to **[6**−$PF_6$**]**$^+$. (b) Calculated isotopic distribution for **[6**−$PF_6$**]**$^+$ (upper) and the amplifying experimental diagram for **[6**−$PF_6$**]**$^+$ (bottom).

(a)

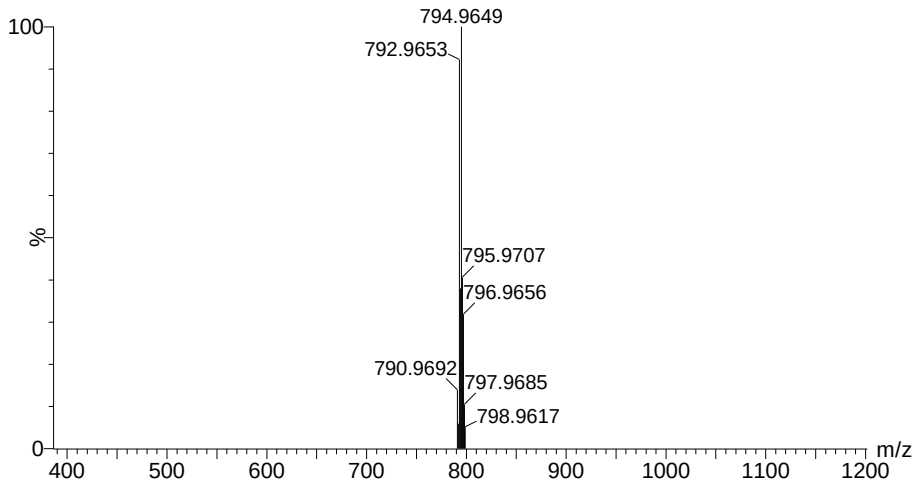


| | | | | | | |
|---|---|---|---|---|---|---|
| Minimum | | | | −1.5 | | |
| Maximum | | 5.0 | 5.0 | 100.0 | | |
| Mass | Calc. Mass | mDa | PPM | DBE | i−FIT | Formula |
| 792.9653 | 792.9674 | -2.1 | -2.6 | 5.5 | 3.1 | C28H46S6Fe2Ag |

(b)

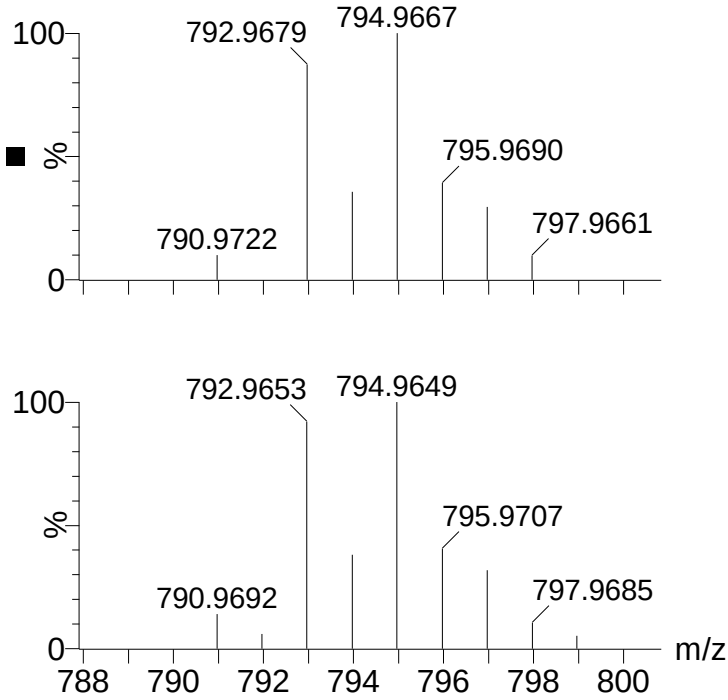

**Figure S12.** ESI-HRMS of **7** in $CH_2Cl_2$.

(a) The signal at an m/z = 802.0865 corresponds to **[7**−$PF_6$**]**$^+$. (b) Calculated isotopic distribution for **[7**−$PF_6$**]**$^+$ (upper) and the amplifying experimental diagram for **[7**−$PF_6$**]**$^+$ (bottom).

(a)

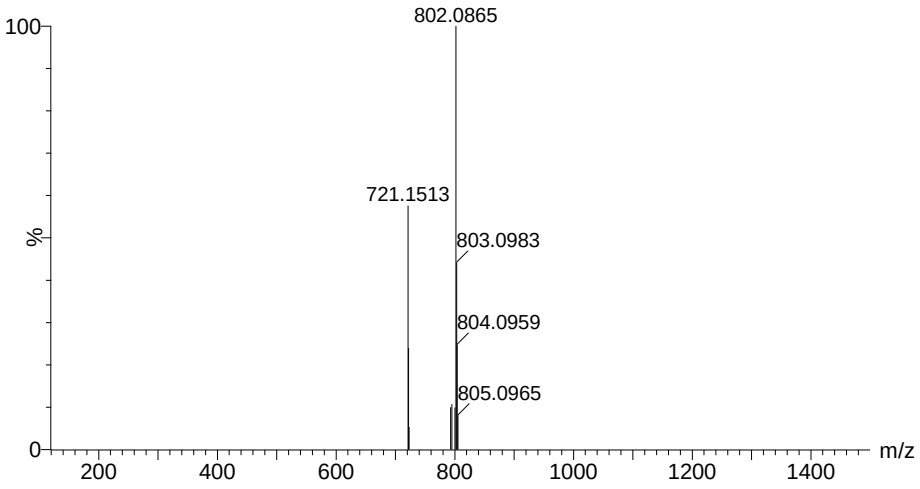


| | | | | | | |
|---|---|---|---|---|---|---|
| Minimum | | | | −1.5 | | |
| Maximum | | 5.0 | 5.0 | 100.0 | | |
| Mass | Calc. Mass | mDa | PPM | DBE | i−FIT | Formula |
| 802.0865 | 802.0888 | -2.3 | -2.9 | 15.0 | 7.0 | C28H38PS3FeAu |

(b)

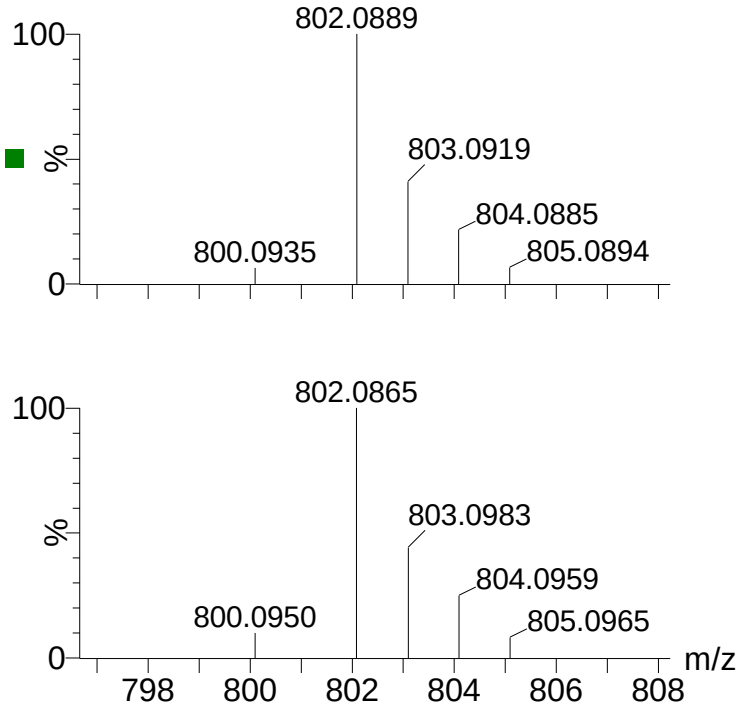

**Figure S13.** The IR (film) spectrum of **2**.

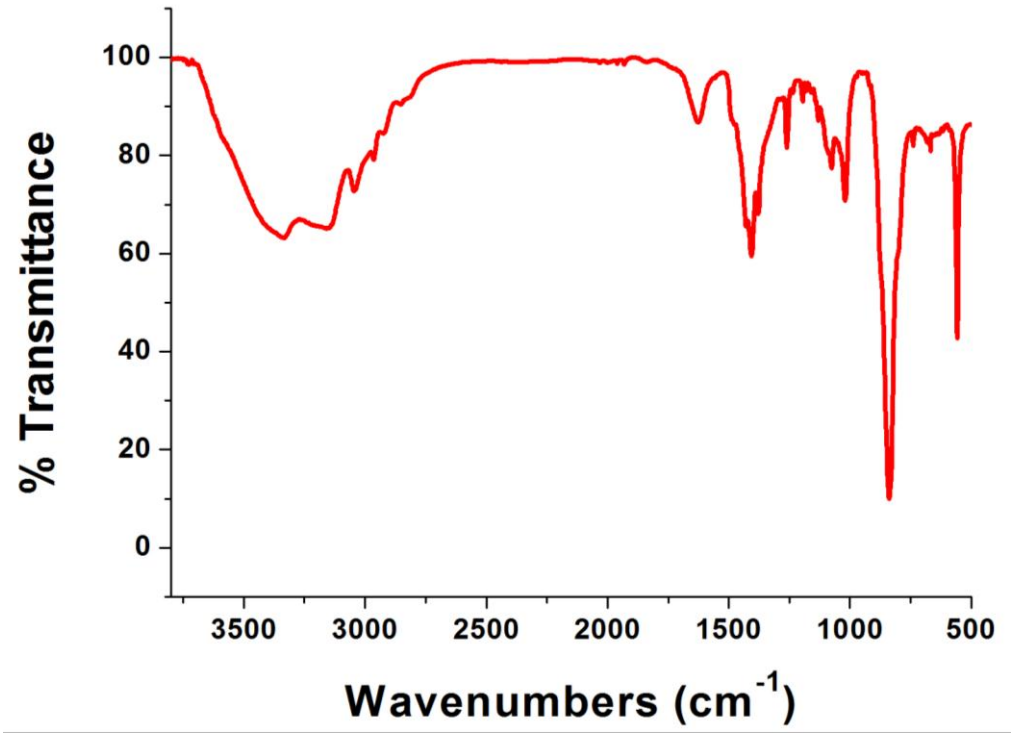


**Figure S14.** The IR (film) spectrum of **3**.

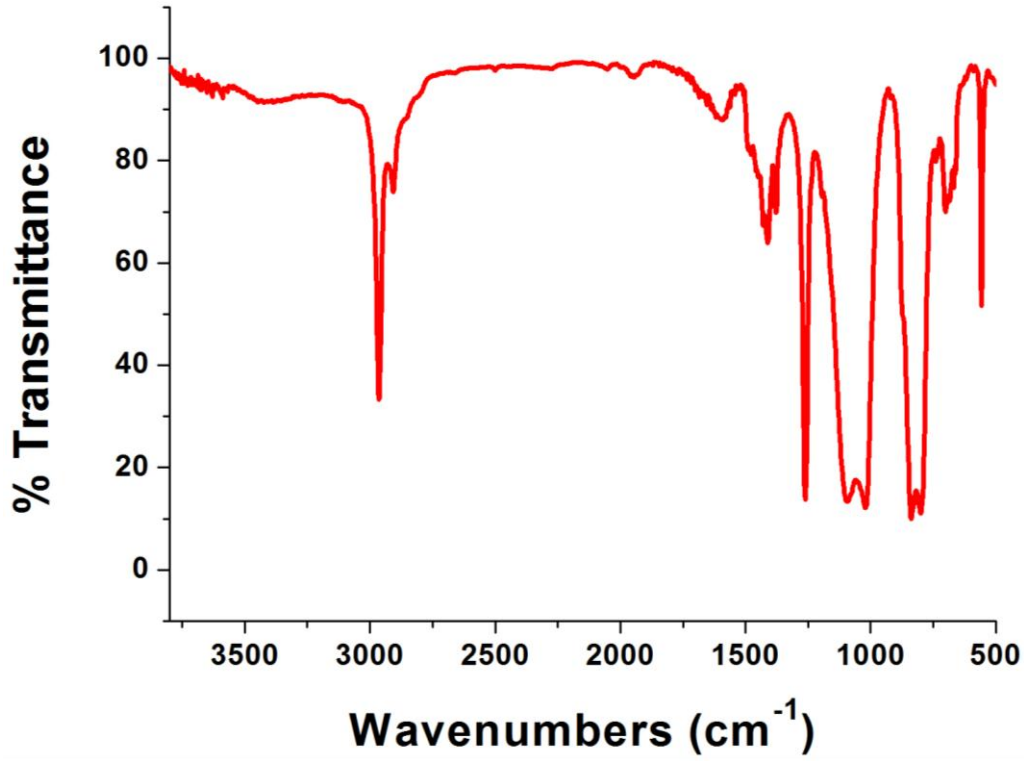

**Figure S15.** The IR (film) spectrum of **4**.

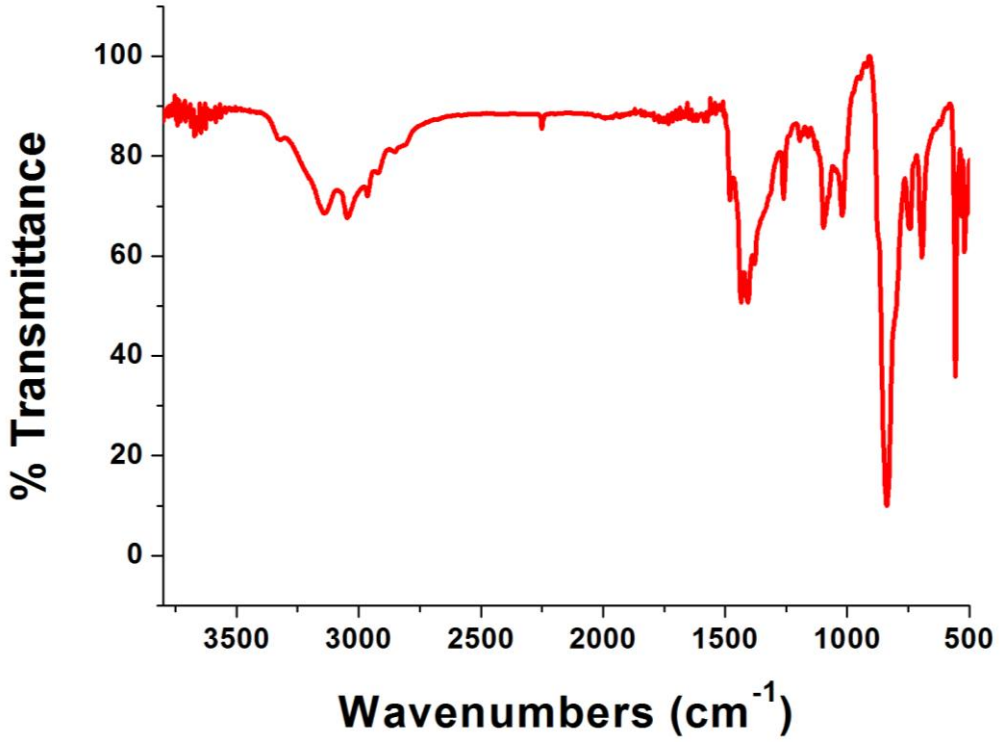


**Figure S16.** The IR (film) spectrum of **5**.

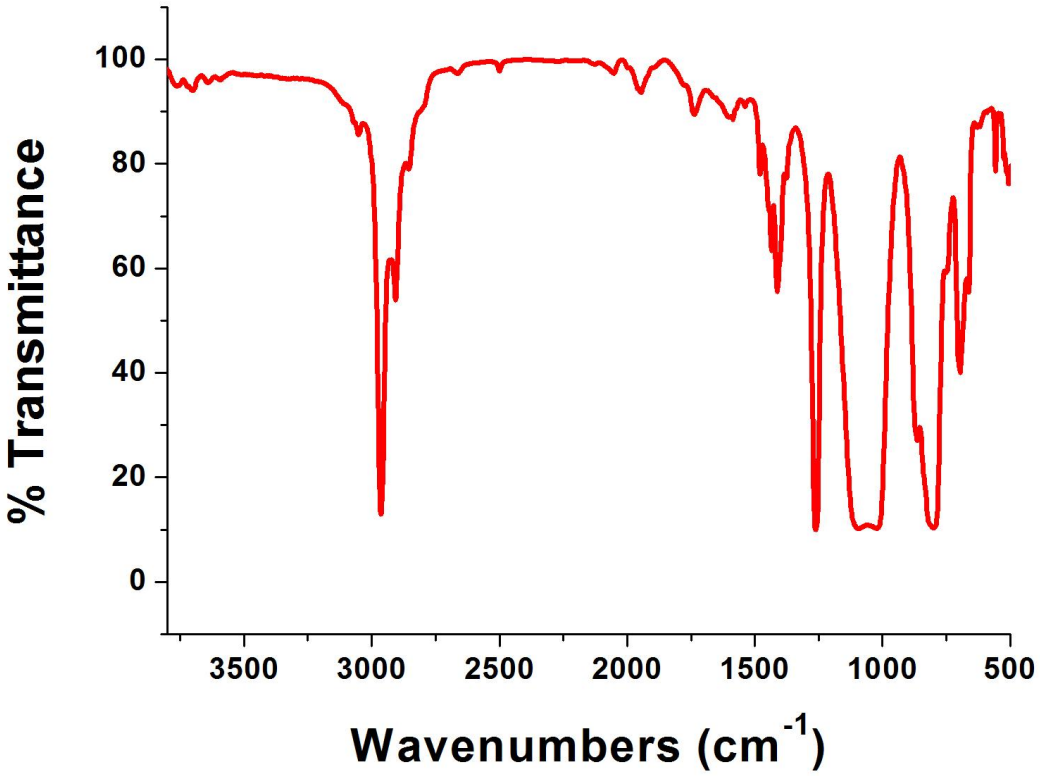

**Figure S17.** The IR (film) spectrum of **6**.

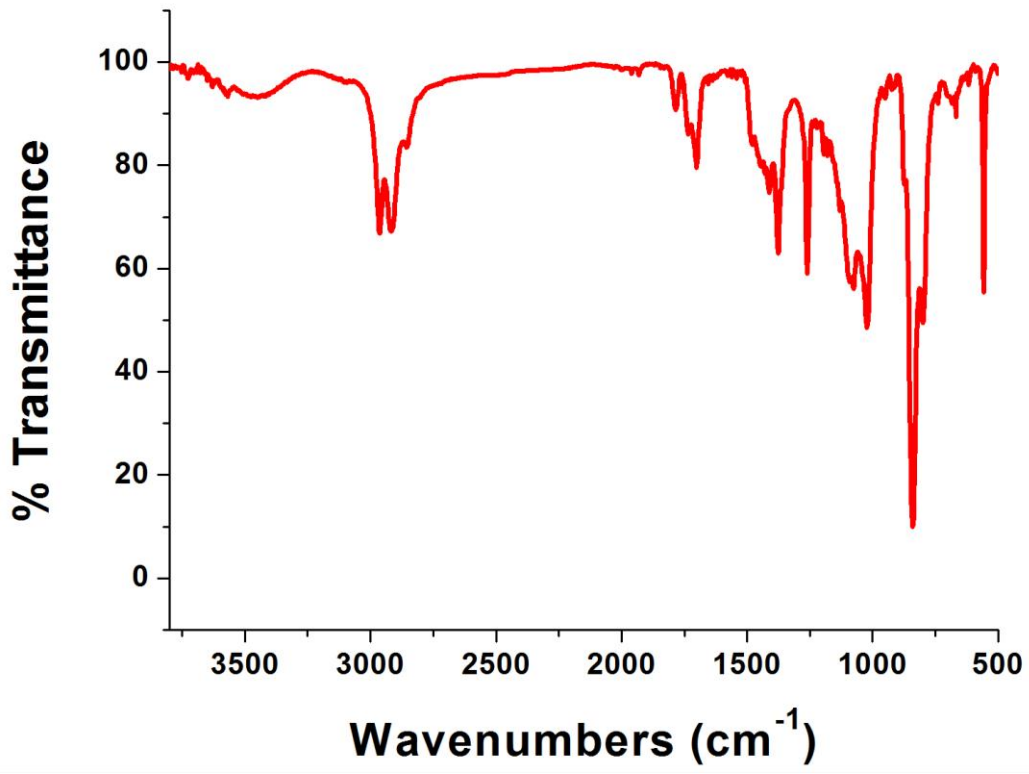


**Figure S18.** The IR (film) spectrum of **7**.

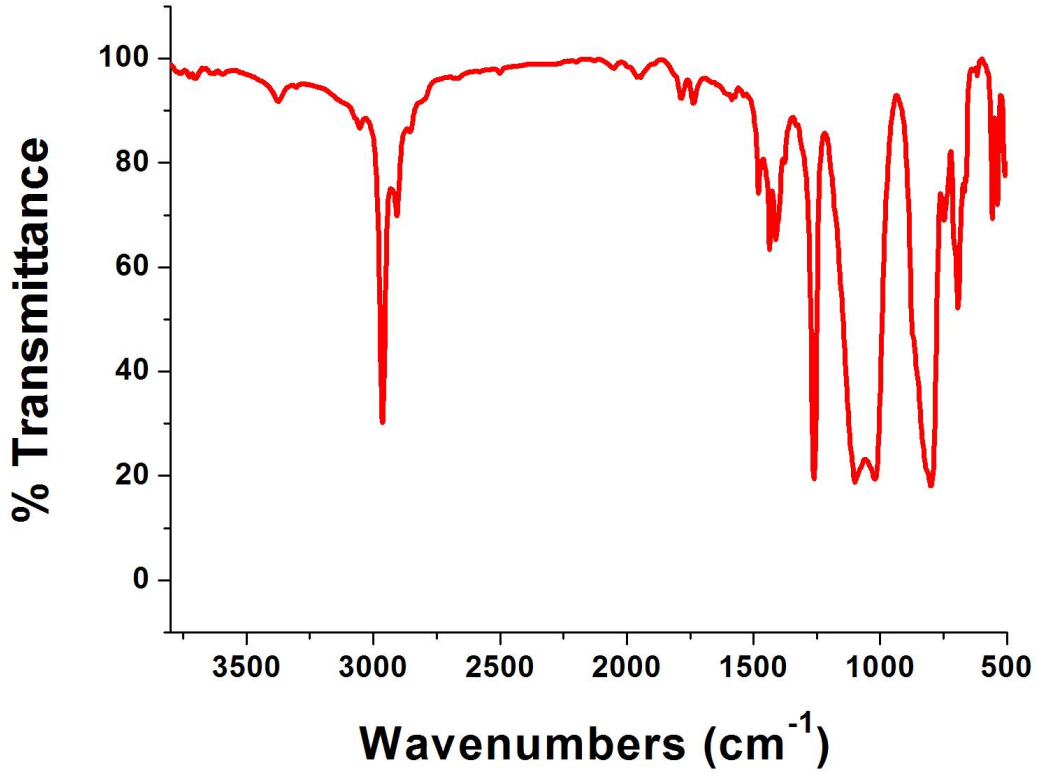

**Figure S19.** The $^{1}H$ NMR spectrum of **2** in $CD_2Cl_2$.

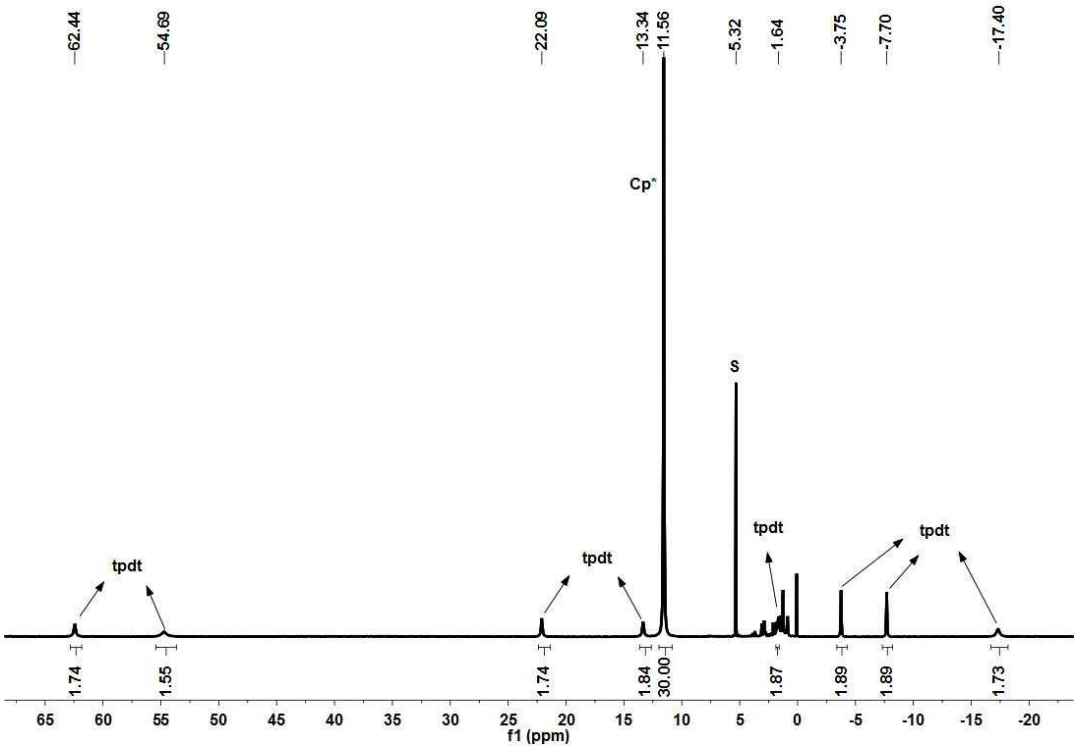


**Figure S20.** The $^{1}H$ NMR spectrum of **3** in $CD_2Cl_2$.

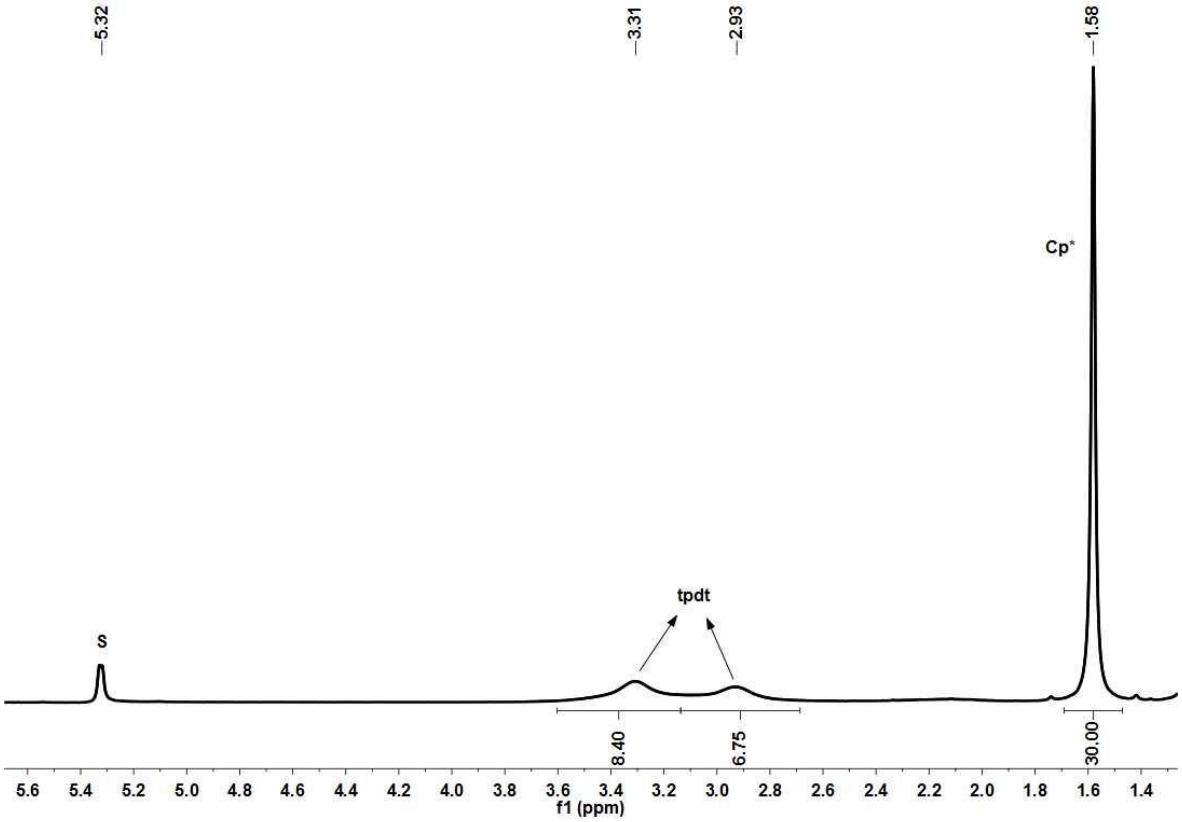

**Figure S21.** The $^1$H NMR spectrum of **4** in $CD_3CN$.

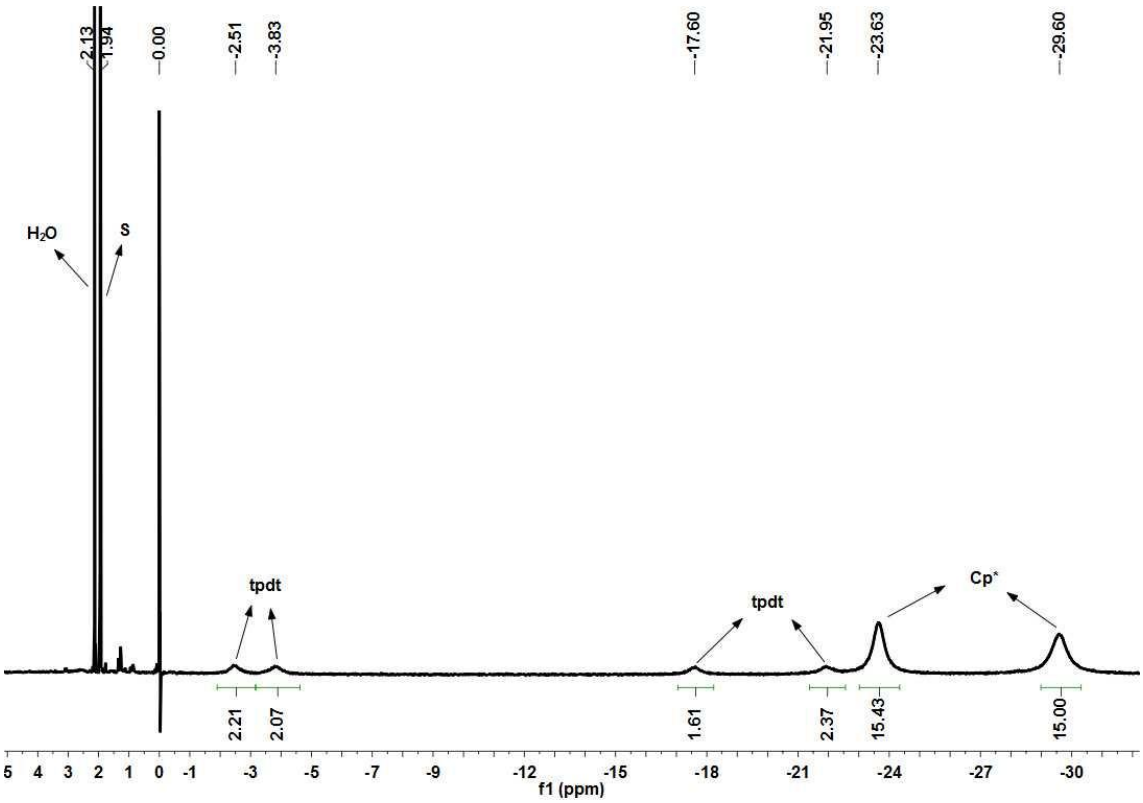


**Figure S22.** The $^1$H NMR spectrum of **5** in $CD_2Cl_2$.

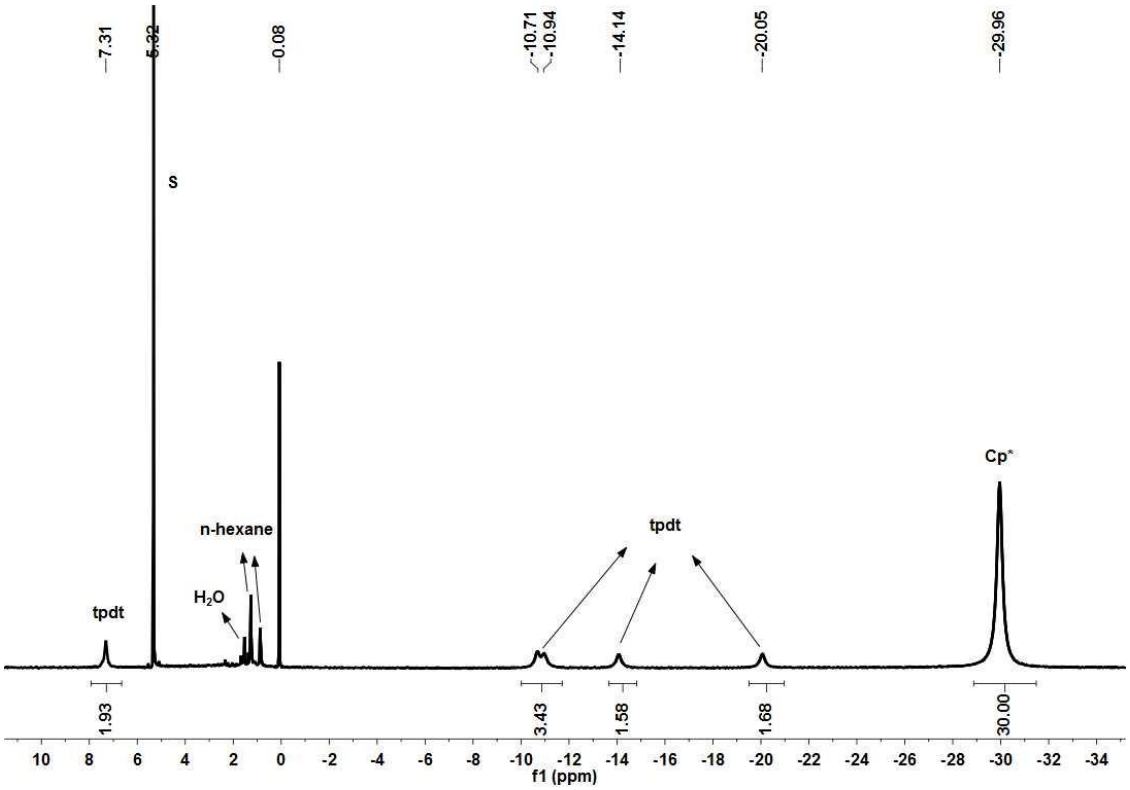

**Figure S23.** The $^1$H NMR spectrum of **6** in $CD_2Cl_2$.

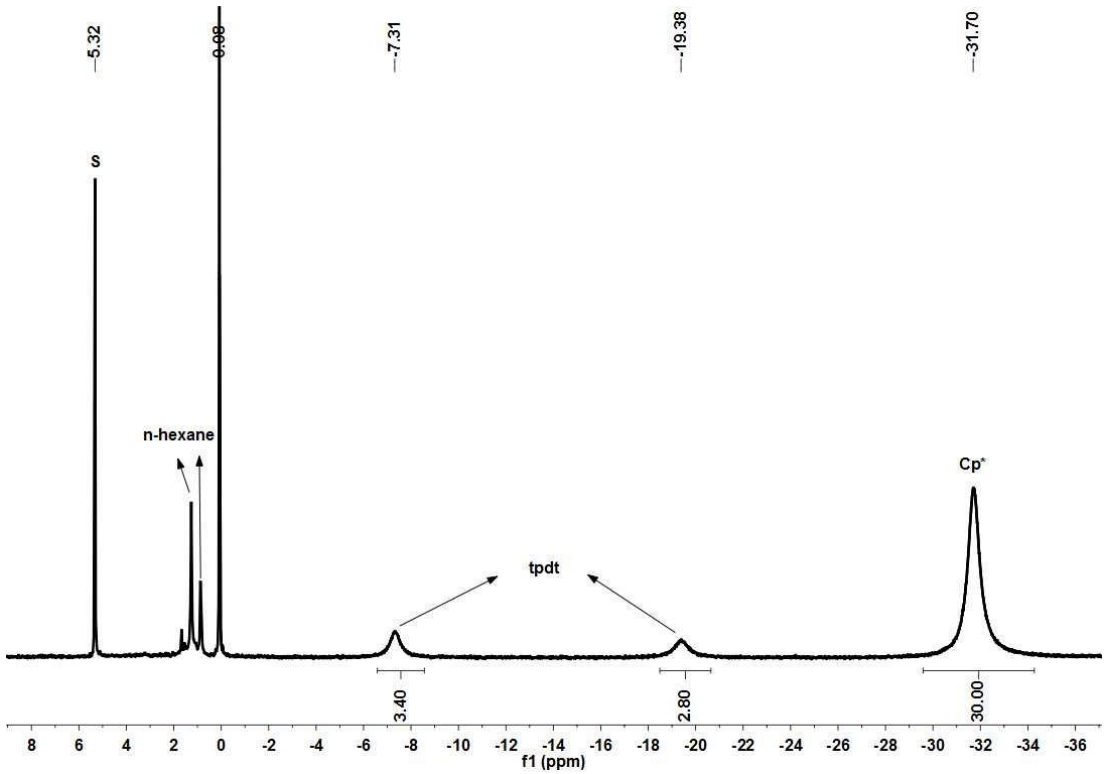


**Figure S24.** The $^1$H NMR spectrum of **7** in $CD_2Cl_2$.

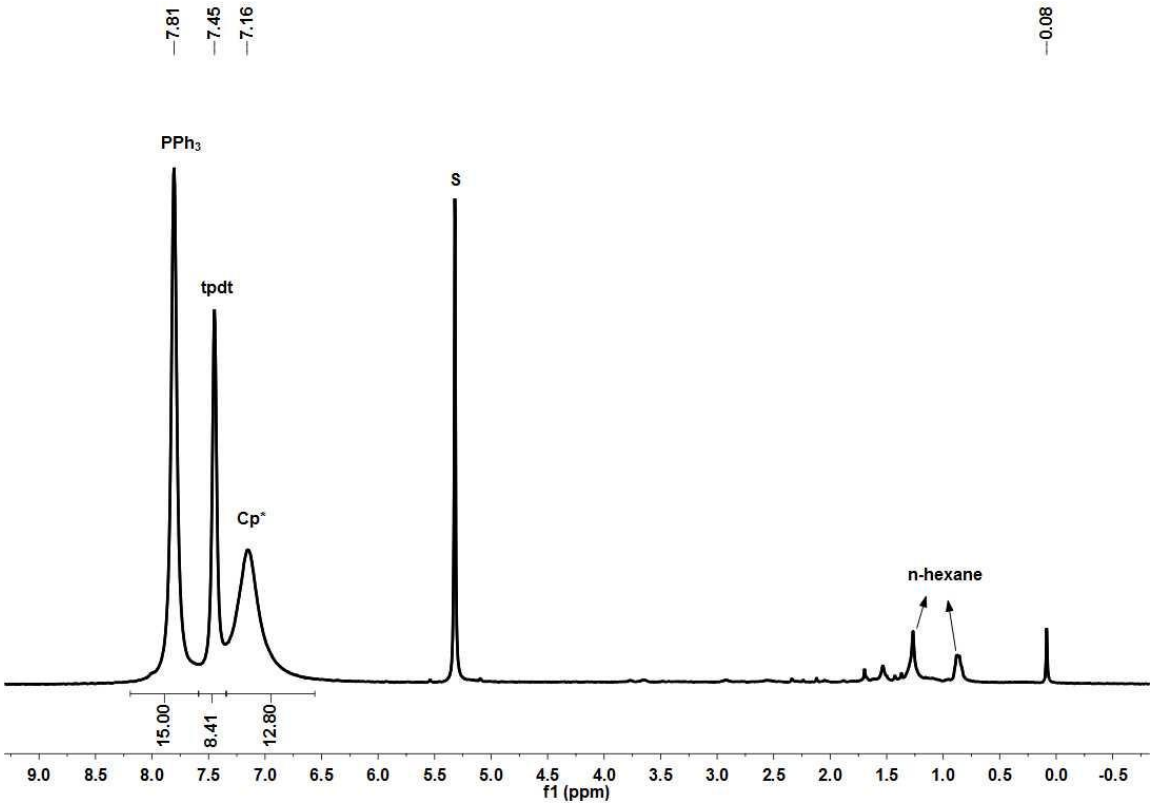

**Figure S25.** The EPR spectrum of **2** at 100 K.

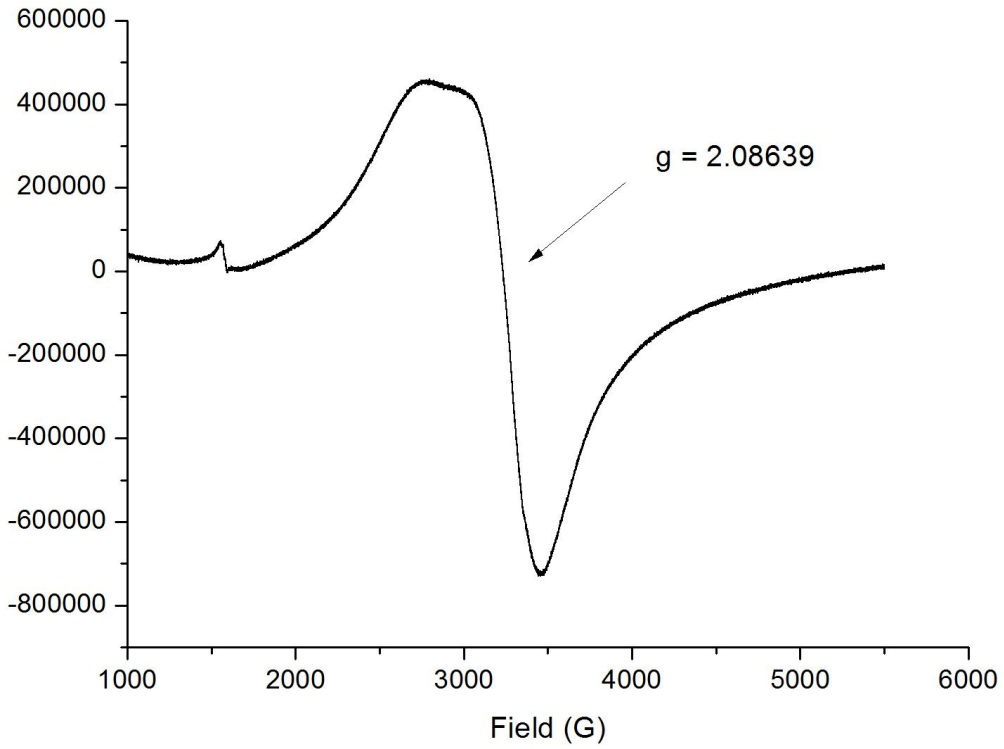


**Figure S26.** The EPR spectrum of **4** at 298 K.

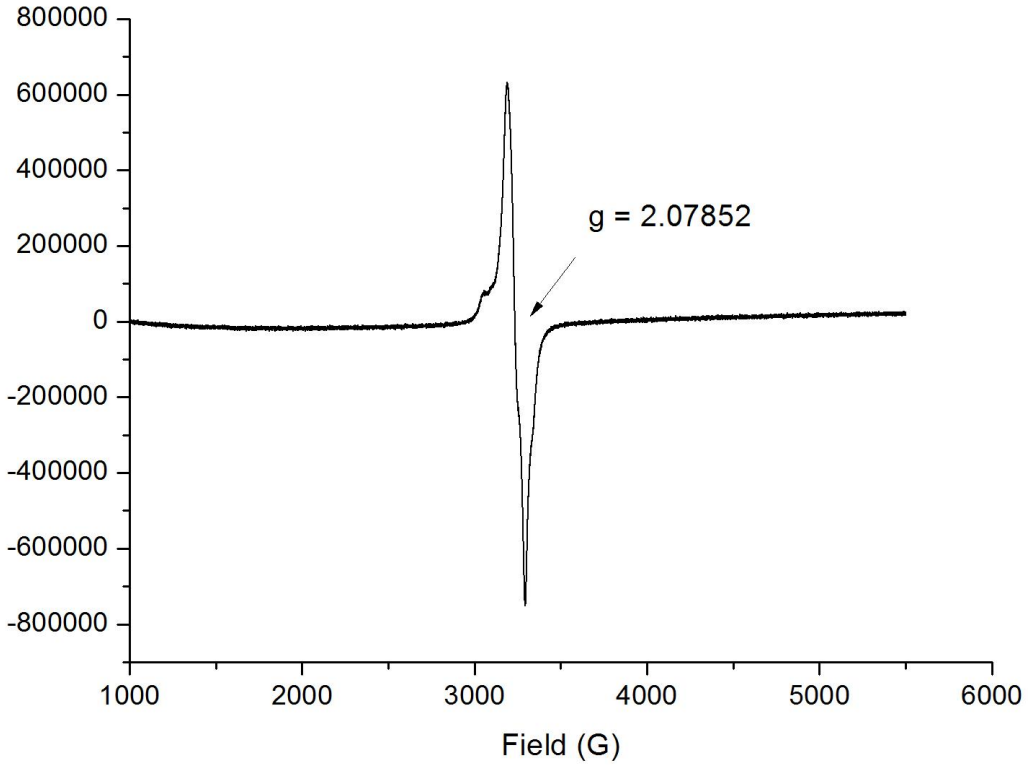

**Figure S27.** The EPR spectrum of **5** at 100 K.

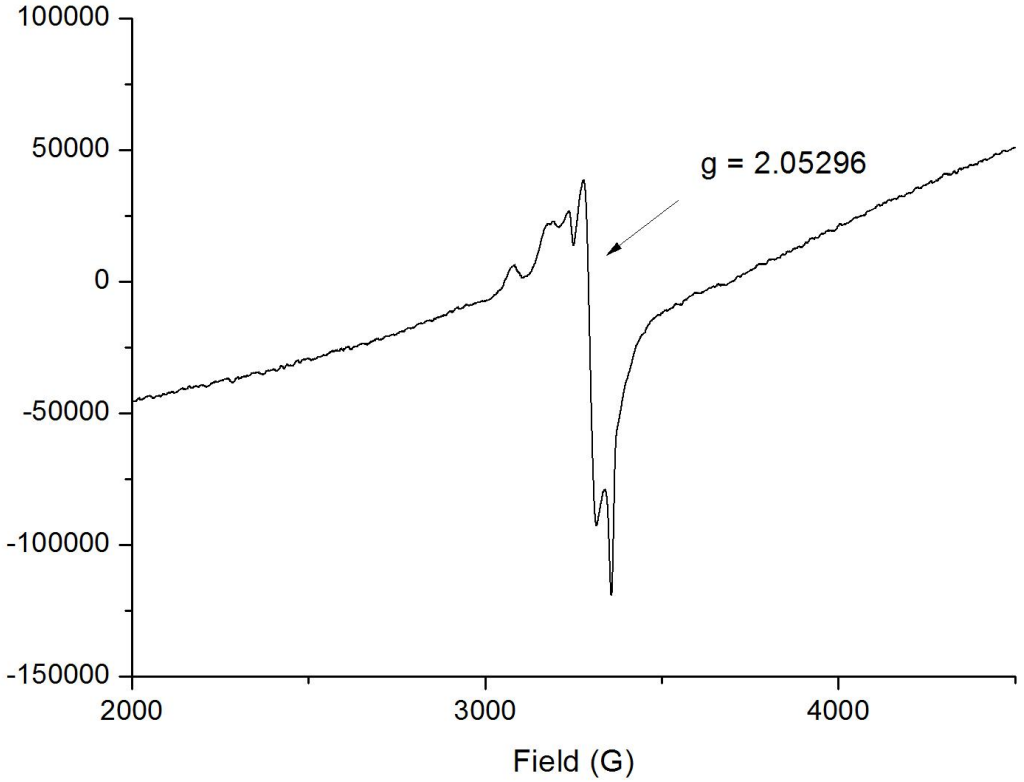


**Figure S28.** The EPR spectrum of **6** at 298 K.

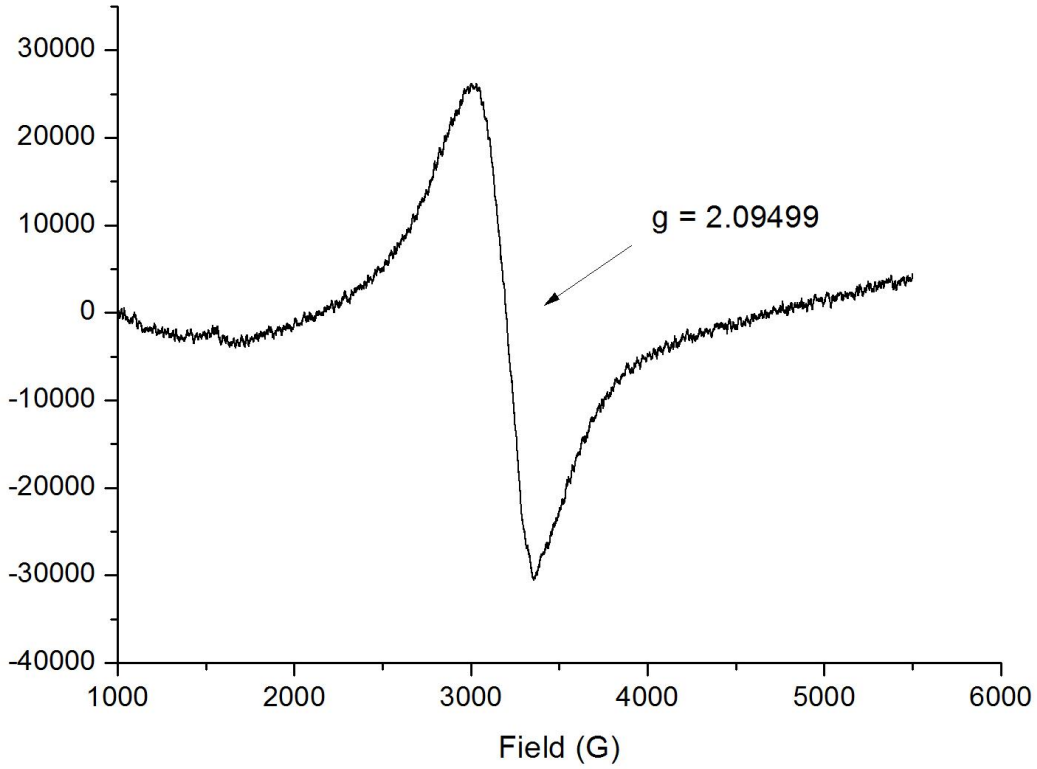

**Figure S29.** The EPR spectrum of **7** at 298 K.

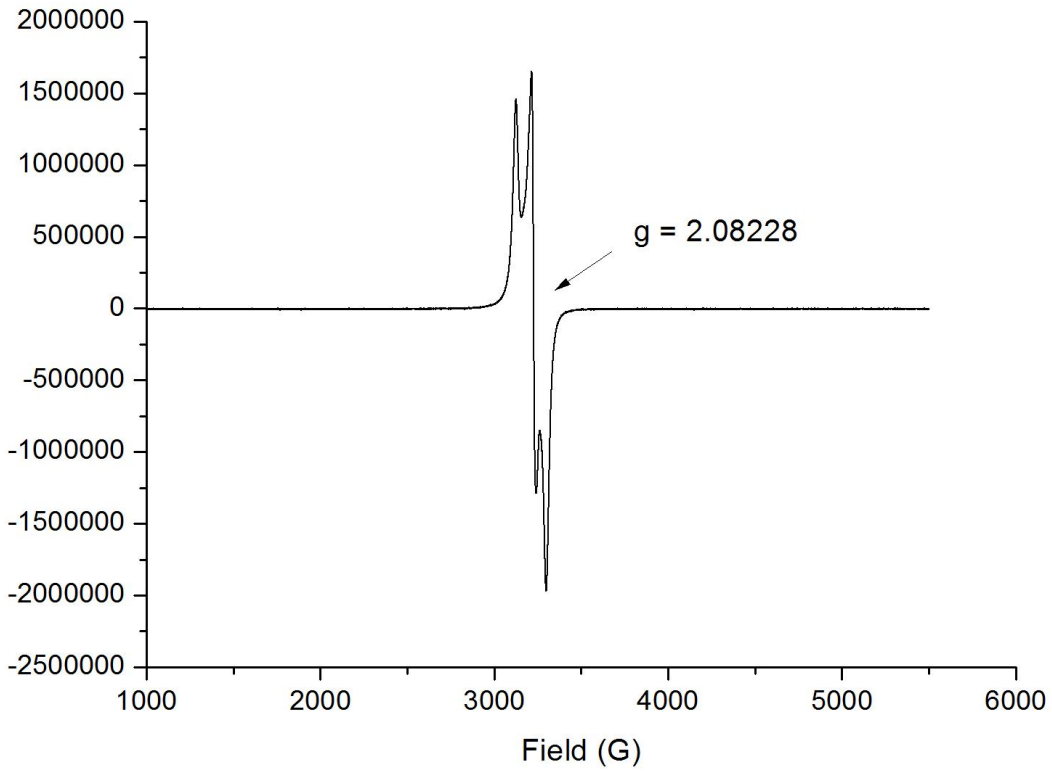


**Figure S30.** The cyclic voltammogram of **2** (1 mM) in 0.1 M $^{n}Bu_4NPF_6/CH_2Cl_2$ at 25 $^{o}$C with a scan rate of 100 mV $s^{-1}$.

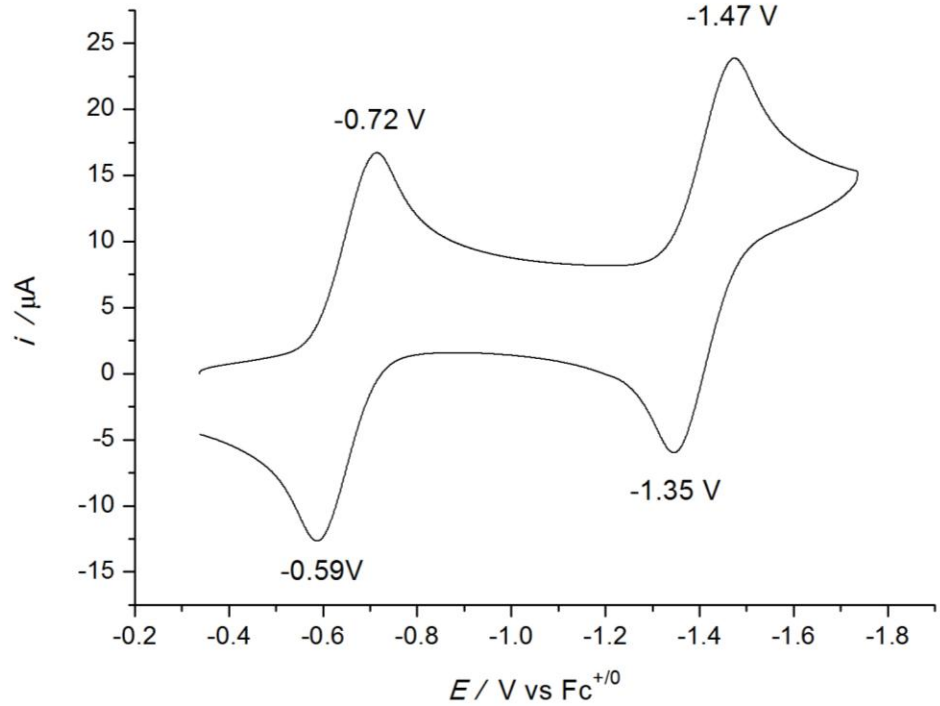

**Figure S31.** The cyclic voltammogram of **3** (1 mM) in 0.1 M $^{n}Bu_4NPF_6/CH_2Cl_2$ at 25 $^{o}$C with a scan rate of 100 mV $s^{-1}$.

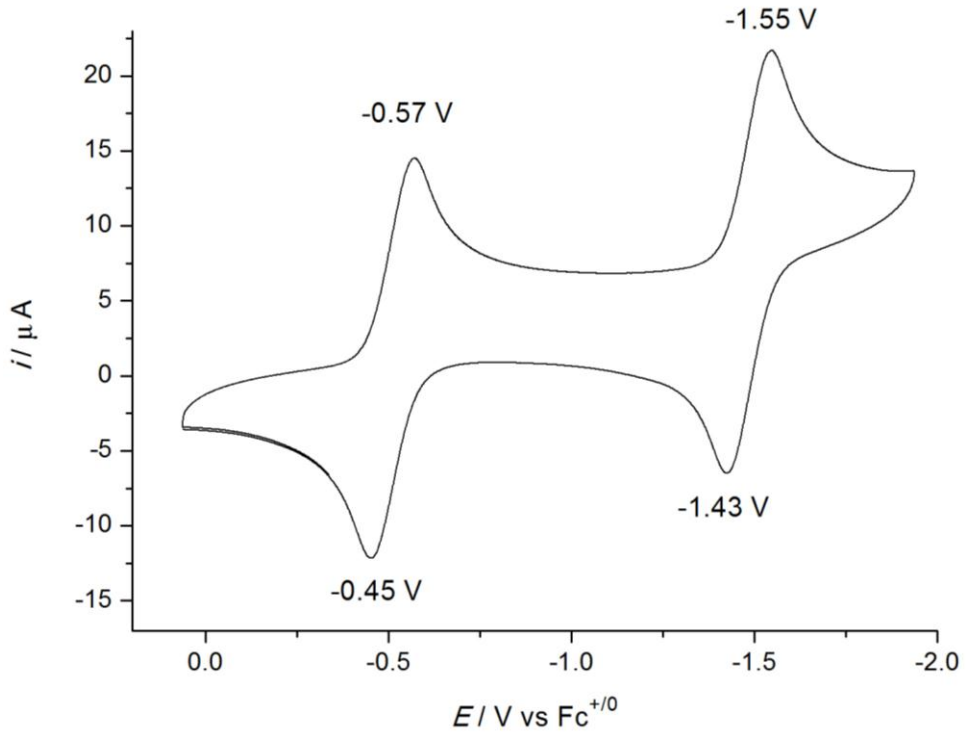


**Figure S32.** The cyclic voltammogram of **4** (1 mM) in 0.1 M $^{n}Bu_4NPF_6$/ $CH_3CN$ at 25 $^{o}$C with a scan rate of 100 mV $s^{-1}$.

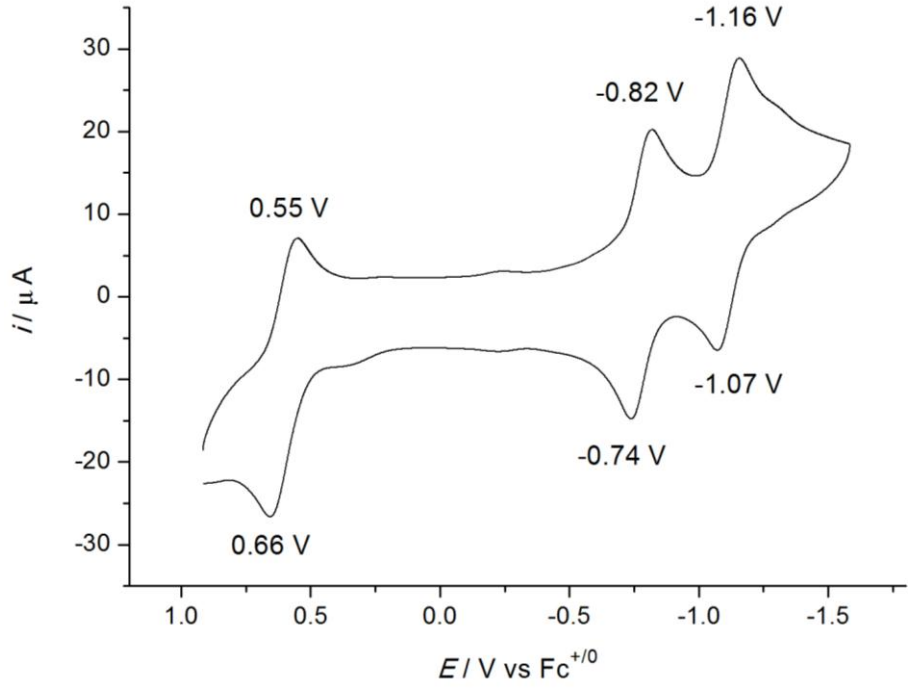

**Figure S33.** The cyclic voltammogram of **5** (1 mM) in 0.1 M $^{n}Bu_4NPF_6$/ $CH_2Cl_2$ at 25 $^{o}$C with a scan rate of 100 mV $s^{-1}$.

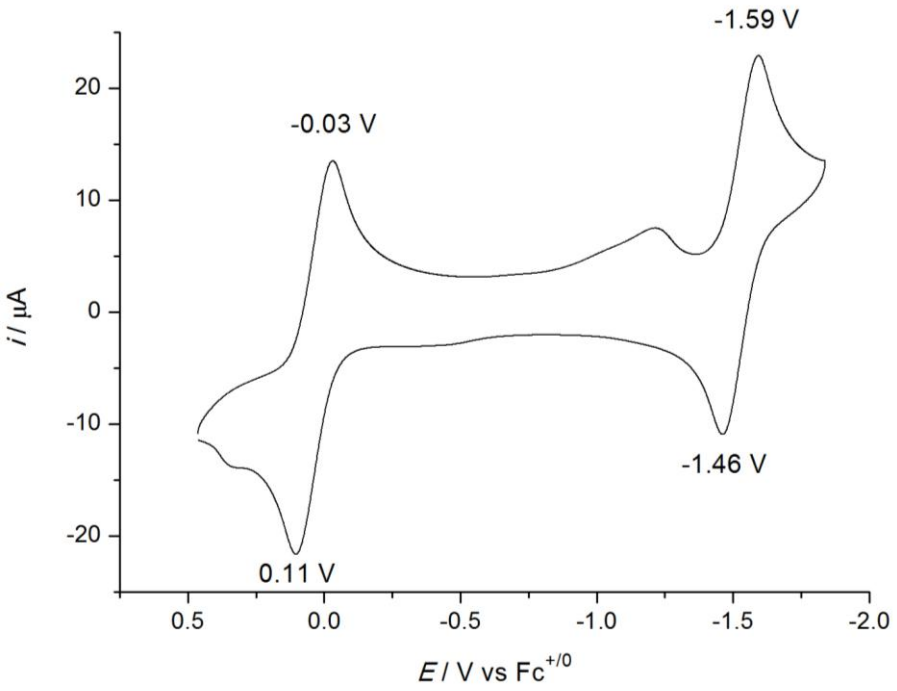


**Figure S34.** The cyclic voltammogram of **6** (1 mM) in 0.1 M $^{n}Bu_4NPF_6$/ $CH_2Cl_2$ at 25 $^{o}$C with a scan rate of 100 mV $s^{-1}$.

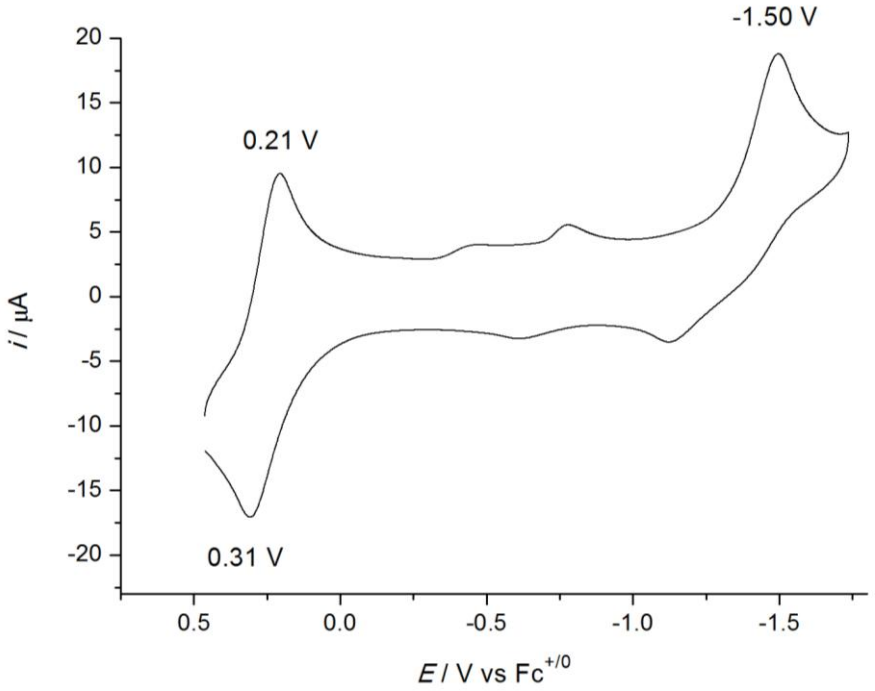

**Figure S35.** The cyclic voltammogram of **7** (1 mM) in 0.1 M $^{n}Bu_4NPF_6$/ $CH_2Cl_2$ at 25 $^{o}$C with a scan rate of 100 mV $s^{-1}$.